INTERNATIONAL JOURNAL OF INTEGRATED ENGINEERING
ISSN: 2229-838X e-ISSN: 2600-7916

IJIE

Vol. 16 No. 5 (2024) 201-213
https://publisher.uthm.edu.my/ojs/index.php/ijie

Redesigning the Omnibus SPRT Control Chart for Simultaneous Monitoring of the Mean and Dispersion of Weibull Processes

J.W. Teoh[1], W.L. Teoh[1]*, Z.L. Chong[2], X.Y. Chew[3], S.Y. Teh[4]

[1] *School of Mathematical and Computer Sciences*
Heriot-Watt University Malaysia, 62200 Putrajaya, MALAYSIA
[2] *Department of Electronic Engineering, Faculty of Engineering and Green Technology*
Universiti Tunku Abdul Rahman, 31900 Perak, MALAYSIA
[3] *School of Computer Sciences*
Universiti Sains Malaysia, 11800 Penang, MALAYSIA
[4] *School of Management*
Universiti Sains Malaysia, 11800 Penang, MALAYSIA

*Corresponding Author: wei_lin.teoh@hw.ac.uk
DOI: https://doi.org/10.30880/ijie.2024.16.05.016

Article Info

Received: 7 December 2023
Accepted: 11 June 2024
Available online: 1 August 2024

Keywords

Average run length, joint monitoring control chart, sequential probability ratio test control chart, skewness correction, standard deviation of the run length, Weibull distribution

Abstract

Quality control charts play an important role in distinguishing between abnormal variations and normal variations of a manufacturing process. Generally, unusual variations in a process may arise due to a change in its mean or dispersion, or a simultaneous change in both parameters. In recent literature, the omnibus sequential probability ratio test (OSPRT) control chart has been proven effective for detecting joint shifts in both the process mean and variability. However, one limitation of the proposed scheme lies in its absolute dependence on the validity of the normality assumption, which may not apply to many quality data, such as machine failure times, the strength of plant fibres, etc. In this research, we critically analyze the performances of the OSPRT chart designed for the Normal distribution, in the case where quality data follow the well-known Weibull distribution. Our findings reveal that the in-control average run length and standard deviation of the run length of the OSPRT chart are significantly compromised due to the positive skewness of the Weibull distribution. As a means of tackling the problem, the skewness correction design has been proposed to correct the control limits of the OSPRT chart. The corrected OSPRT chart is found to produce a more satisfactory in-control performance, with an acceptable decline in its sensitivity towards small process shift sizes.

1. Introduction

Statistical quality control (SQC) is a vital aspect of every modern manufacturing and service industry. It plays a pivotal role in ensuring the consistency of products or processes, allowing organizations to identify variations and make informed decisions for process improvement. One powerful tool within the realm of SQC is the control chart. Control charts provide a graphical representation of process data over time, enabling practitioners to distinguish between common cause and special cause variations [1-3]. Common cause variations are small variations that are inherent to each process, whereas special cause variations are unusual variations that arise from unsolicited events, such as machine failure, change in environmental factors, etc [1]. Generally, organizations aim to detect and eliminate special cause variations as quickly as possible to avoid losses due to

This is an open access article under the CC BY-NC-SA 4.0 license.

suboptimal production. By utilizing control charts, organizations gain a real-time understanding of process stability and performance, hence facilitating timely interventions to prevent defects and enhance overall quality. Many recent research studies have focused on the development of time-weighted control charts, as these control charts are designed to account for the impact of time on the data points, thus providing a more accurate representation of a process's performance. Some excellent examples include the analysis conducted by You et al. [4] on the performances of the side sensitive group runs chart and the exponentially weighted moving average (EWMA) chart, the development of a self-starting non-restarting cumulative sum (CUSUM) control chart by Mou et al. [5], the modified run sum *t* control chart with an extra variable sampling interval feature by Mim et al. [6], to name a few.

Joint monitoring of both the mean and dispersion within a process is imperative to achieve and sustain high-quality outputs. The mean, which is a measure of central tendency, provides a crucial benchmark for meeting product specifications and customer expectations. Cautious monitoring of the process mean allows practitioners to quickly identify any shifts that might compromise the quality of outputs. Simultaneously, monitoring of the process variability, whether through the standard deviation or range, offers insights into the stability and consistency of a process. Fluctuations in the variability can be indicative of changes in the production environment, the introduction of new materials, or other factors affecting the uniformity of the process. Many recently proposed control charts are equipped with such functionalities, see for example, the maximum weighted adaptive Crosier CUSUM chart [7], the EWMA likelihood ratio chart with double ranked set sampling [8], the maximum triple EWMA chart [9], and the omnibus sequential probability ratio test (OSPRT) chart [10]. While the CUSUM and EWMA charts have remained popular choices of control charts since the past few decades, there has been increasing attention garnered by the sequential probability ratio test (SPRT) chart. Particularly, references [10-13] showed that the SPRT chart outperforms Shewhart-type and CUSUM charts in terms of the average detection speed from many aspects (e.g., the mean and standard deviation shifts). The OSPRT chart, which is developed for simultaneous monitoring of the process mean and dispersion, is found to be optimum for detecting any deterministic joint shift sizes when the quality variable assumes the Normal distribution [10]. Teoh et al. [10] showed that the OSPRT chart has a superior performance over the Shewhart $\bar{X}$-S, weighted-loss CUSUM, and absolute value SPRT control charts in terms of the average detection speed. In particular, they showed that the OSPRT chart outperforms the Shewhart $\bar{X}$-S and weighted-loss CUSUM charts by over 100% and outperforms the absolute value SPRT chart by percentages ranging from 6% to 110%. Besides, the OSPRT chart possesses the advantage of sampling only a small number of observations on average to reach a decision, thus offering a significant saving in terms of the inspection and sampling costs. This property makes the OSPRT chart extremely appealing in applications where destructive testing is dominant, as compared to other joint monitoring control schemes based on fixed sample sizes. In this paper, we focus entirely on the OSPRT scheme.

The OSPRT scheme was originally designed for detecting changes in the parameters of Normal distributed variables. However, according to Li et al. [14], certain data, such as time-between-events data, are best modelled by the Weibull distribution. This stems from the fact that the Weibull distribution has a flexible structure for modelling times between system failures. Some other process characteristics that can be adequately described by a Weibull distribution include the kenaf fiber tensile strength [15], the wind velocity [16], the mean time between failures of machines [17], etc. It is frequently documented that control charts designed for the Normal distribution tend to perform poorly under non-Normal conditions, see for example, [18-20]. Many researchers have identified a significant reduction in the in-control average run length (ARL), which means that practitioners are likely to encounter higher levels of false alarms when data are positively skewed. As a remedy, researchers have proposed two different methods to counter the effects of non-normality on the performances of control charts. The first method involves developing a new parametric or nonparametric control chart that is robust towards non-Normal distributions, see for example [20-22]. This method requires significant theoretical effort, since developing a new type of statistic or control strategy is often not easy. In some cases, the control chart may lose its power as a result of adopting a nonparametric statistic, when the underlying data indeed follow the Normal distribution. The second method involves correcting the control limits of the control chart according to the skewness of the data [19, 23, 24]. The adjusted or corrected control limits are determined by ensuring that the recommended in-control ARL is satisfied, with minimum changes made to the original features of the control chart. This method may be preferred in cases when practitioners wish to retain most of the original features of a control chart. In this paper, we study the performances of the OSPRT chart designed for the Normal distribution, when the underlying data follow the Weibull distribution. We also propose a new skewness correction method for the OSPRT chart based on various degrees of skewness.

The structure of the paper is detailed as follows. In Section 2, we describe the methodologies used in our research, which comprise a brief review of the OSPRT chart, its run-length properties, as well as the statistical properties of the Weibull distribution. In Section 3, we evaluate the ARL and standard deviation of the run length (SDRL) of the OSPRT chart designed for the Normal distribution, under conditions where the Weibull distribution is assumed. The results obtained are then compared with those obtained under the usual Normal distribution to emphasize the necessity of developing a correction strategy for the OSPRT chart. Next, we

Int. Journal of Integrated Engineering Vol. 16 No. 5 (2024) p. 201-213

provide a complete framework for calculating the adjusted control limits of the OSPRT chart based on the skewness correction method. Finally, some concluding remarks and future research directions are given.

2. Methodology

2.1 Background of The OSPRT Chart

Let ($Y_{1,1}$, $Y_{1,2}$, …, Y_{1,N_1}), ($Y_{2,1}$, $Y_{2,2}$, …, Y_{2,N_2}), … be a sequence of measurements obtained from a process that follows the Normal distribution with mean μ_0 and standard deviation σ_0, where N_1, N_2, … are the numbers of measurements taken in each sample. As sampling is done at random, it is reasonable to assume that the measurements are independent of each other. It is further assumed that measurements from the same sample (i.e., $Y_{i,1}$, $Y_{i,2}$, … for i = 1, 2, …) are acquired within a negligible time frame. The OSPRT scheme for detecting a change in the parameter vector from (μ_0, σ_0) to ($\mu_0 + \delta\sigma_0$, $\eta\sigma_0$) has the control statistic

$$T_{i,j} = \operatorname{sgn}(\eta - 1)\sum_{j'=1}^{j}\left[\left(\frac{Y_{i,j'} - \mu_0}{\sigma_0} + k\right)^2 - \gamma\right], \tag{1}$$

for i = 1, 2, …, and j = 1, 2, …, N_i, where N_i represents the number of measurements required by the ith OSPRT, δ and η represent the magnitudes of the shifts in the process mean and standard deviation, respectively. In Equation (1), sgn(η − 1) represents the sign of the quantity (η − 1), $Y_{i,j'}$ is the j'th measurement in the ith sample, k and γ represent the reference parameters of the OSPRT scheme. It is shown that the out-of-control ARL (ARL_1) can be minimized by setting the reference parameters to

$$k = \frac{\delta}{\eta^2 - 1} \tag{2}$$

and

$$\gamma = \frac{\delta^2\eta^2}{(\eta^2 - 1)^2} + \frac{2\eta^2}{\eta^2 - 1}\ln(\eta), \tag{3}$$

respectively [10]. Teoh et al. [10] argued that an increasing shift in the process variability is much more endangering than a decreasing shift in the variability. Hence, in this paper, we consider only the case $\eta > 1$, which means that sgn(η − 1) equals 1 in Equation (1). It should be noted from Equation (2) that, when $\delta > 0$, $k > 0$; whereas when $\delta < 0$, $k < 0$. As the OSPRT scheme for $\delta > 0$ is identical to that for $\delta < 0$, we shall restrict our study to only the case $\delta > 0$.

The operation of the OSPRT chart is similar to those of the other SPRT control charts, e.g., the SPRT chart for the process mean and the SPRT chart for the process variance. There are two control limits for the OSPRT chart, i.e., the lower control limit g and the upper control limit h. The decision criteria of the OSPRT scheme can be separated into three different cases:

Case 1: If the control statistic $T_{i,j}$ exceeds the upper control limit h, the measurements are said to come from an out-of-control process. Sampling is terminated.

Case 2: If the control statistic $T_{i,j}$ goes below the lower control limit g, the measurements are said to come from an in-control process. Sampling is terminated.

Case 3: If the control statistic $T_{i,j}$ lies in the region between g and h, there is nothing we can conclude about the process. Sampling is resumed.

In Case 1, since the process is identified as problematic, a designated out-of-control action plan should be executed in order to identify the root cause of the issue and eliminate it as soon as possible. In Case 2, since the process is declared as in-control, the process will be continuously assessed at regular time intervals until an out-of-control signal is given.

2.2 Run-length Properties of The OSPRT Chart

Practitioners are often interested in understanding how a control chart performs in charting applications, e.g., how many samples it takes to identify a process shift, how many observations are depleted during the inspection, etc. In this paper, we evaluate three run-length properties of the OSPRT chart, i.e., the ARL, SDRL, and the average sample size (ASS). These properties are evaluated via the Markov chain approach. Suppose the charting region [g, h] is divided into L subintervals, each of width $\Delta = (h - g)/L$. The sequence of subintervals, i.e., (g, $g + \Delta$), ($g + \Delta$, $g + 2\Delta$), ……, ($g + (L - 1)\Delta$, h), can be interpreted as the transient states of the Markov chain. Suppose further that the regions ($-\infty$, g] and [h, ∞) represent the absorbing states of the Markov chain, i.e., the control statistic stops moving after it falls into either ($-\infty$, g] and [h, ∞). To calculate the performance metrics of

the OSPRT chart, we need to set up a matrix **Q** that contains the transition probabilities for each of the L transient states. Let $q_{a,b}$ denote the one-step transition probability from the ath state to the bth state. To derive an approximate expression for $q_{a,b}$, we assume that the control statistic lies on the midpoint of the ath state initially, i.e., the initial value of the control statistic $T_{i,j} = g + (a - 0.5)\Delta$. The expression for $q_{a,b}$ is given as

$$q_{a,b} = \chi^2_{(\delta+k)^2/\eta^2,1}\left[\frac{\gamma+(b-a+0.5)\Delta}{\eta^2}\right] - \chi^2_{(\delta+k)^2/\eta^2,1}\left[\frac{\gamma+(b-a-0.5)\Delta}{\eta^2}\right], \tag{4}$$

for a, b = 1, 2, ..., L, where $\chi^2_{(\delta+k)^2/\eta^2,1}(\cdot)$ represents the cumulative distribution function (cdf) of the non-central chi-squared distribution with one degree of freedom and non-centrality parameter $(\delta + k)^2/\eta^2$. The complete proof of derivation can be found in Teoh et al. [10].

In the following step, we define the one-step transition probability d_a from the initial state to the ath transient state as follows:

$$d_a = \chi^2_{(\delta+k)^2/\eta^2,1}\left[\frac{\gamma+g+a\Delta}{\eta^2}\right] - \chi^2_{(\delta+k)^2/\eta^2,1}\left[\frac{\gamma+g+(a-1)\Delta}{\eta^2}\right]. \tag{5}$$

The probability defined above is encoded in a column vector **D** with L entries. The ASS of the OSPRT chart can then be derived as [10]

$$\text{ASS} = 1 + \mathbf{D}^{\mathrm{T}}(\mathbf{I} - \mathbf{Q})^{-1}\mathbf{1} \tag{6}$$

using the fundamental matrix of the absorbing Markov chain. Here, **I** is a unit matrix and **1** is a column vector whose entries are filled with ones.

To derive the expressions for the ARL and SDRL, we first construct a vector **C** that contains the transition probabilities from the L transient states to the acceptance state (i.e., the region below g). The one-step transition probability from the ath transient state to the acceptance state is given as

$$c_a = \chi^2_{(\delta+k)^2/\eta^2,1}\left[\frac{\gamma+(0.5-a)\Delta}{\eta^2}\right]. \tag{7}$$

Next, we define the one-step transition probability from the initial state to the acceptance state as follows:

$$P_0 = \chi^2_{(\delta+k)^2/\eta^2,1}\left(\frac{\gamma+g}{\eta^2}\right). \tag{8}$$

The probability that the control statistic eventually lands on the in-control region (i.e., acceptance state), conditional on the joint shift sizes (δ, η), has the formula:

$$P(\delta,\eta) = P_0 + \mathbf{D}^{\mathrm{T}}(\mathbf{I} - \mathbf{Q})^{-1}\mathbf{C}\,. \tag{9}$$

Note that Equation (9) is also referred to as the operating characteristic function of the OSPRT chart.

Since the ARL and SDRL measure the average and the standard deviation of the number of samples up to the point where the control statistic falls in the out-of-control region (i.e., region above h), we can derive their formulae as

$$\text{ARL} = \frac{1}{1 - P(\delta,\eta)} \tag{10}$$

and

$$\text{SDRL} = \sqrt{\frac{P(\delta,\eta)}{\left[1 - P(\delta,\eta)\right]^2}}, \tag{11}$$

respectively, by using the properties of a geometric distribution.

Int. Journal of Integrated Engineering Vol. 16 No. 5 (2024) p. 201-213

2.3 Statistical Properties of The Weibull Distribution

In this section, we present the formulae for the statistical properties of the Weibull distribution, i.e., the mean (μ_0^w), standard deviation (σ_0^w), and the coefficient of skewness (θ). The probability density function of the Weibull distribution is

$$f_X(x) = \frac{\beta}{\lambda}\left(\frac{x}{\lambda}\right)^{\beta-1} \exp\left\{-\left(\frac{x}{\lambda}\right)^{\beta}\right\}, \tag{12}$$

for $x \geq 0$, where $\beta > 0$ and $\lambda > 0$ are the shape and scale parameters of the Weibull distribution, respectively. The cdf of the Weibull distribution is

$$F_X(x) = 1 - \exp\left\{-\left(\frac{x}{\lambda}\right)^{\beta}\right\}. \tag{13}$$

It is worth noting that the skewness of the Weibull distribution does not depend on the scale parameter λ. Hence, we set $\lambda = 1$ throughout this paper for the ease of computation. The formulae for the mean, standard deviation, and coefficient of skewness of the Weibull distribution are expressed as [25]

$$\mu_0^w = \Gamma\left(1+\frac{1}{\beta}\right), \tag{14}$$

$$\sigma_0^w = \sqrt{\Gamma\left(1+\frac{2}{\beta}\right) - \Gamma^2\left(1+\frac{1}{\beta}\right)}, \tag{15}$$

and

$$\theta = \frac{\Gamma\left(1+\frac{3}{\beta}\right) + 2\Gamma^3\left(1+\frac{1}{\beta}\right) - 3\Gamma\left(1+\frac{1}{\beta}\right)\Gamma\left(1+\frac{2}{\beta}\right)}{\left[\Gamma\left(1+\frac{2}{\beta}\right) - \Gamma^2\left(1+\frac{1}{\beta}\right)\right]^{1.5}}, \tag{16}$$

respectively.

3. Results and Discussions

3.1 Adverse Effects of Skewness on The Performances of The OSPRT Chart Under The Weibull Distribution

To evaluate the impact of skewness on the performances of the OSPRT chart, we first describe the framework for designing the OSPRT chart under the Normal distribution. At the outset, practitioners must specify two design parameters for the OSPRT chart, i.e., the recommended in-control ARL (ARL_0) (τ) and the desired in-control ASS (ASS_0) (n). Practitioners then decide which combination of reference parameters (k, γ) and control limits (g, h) are appropriate for the OSPRT chart based on the two specifications mentioned earlier. Teoh et al. [10] showed that k and γ can be taken as the independent parameters of the design, whereas g and h are dependent parameters whose values are adjusted to satisfy the two specifications mentioned earlier. In this section, we set the design parameters as $\tau = 370.4$ and $n = 5$, and we present results for four different combinations of (k, γ), i.e., (k, γ) ∈ {(0.1, 2.0), (0.1, 5.0), (0.5, 2.5), (0.5, 6.0)}. Note that the control limits g and h are calculated by setting the constraints $ARL_0 = \tau = 370.4$ and $ASS_0 = n = 5$. Deore et al. [12] stated that the value of g is mostly affected by changes in the ASS_0, whereas the value of h is mostly affected by changes in the ARL_0. Hence, the values of g and h are adjusted in turn to satisfy the constraints $ARL_0 = 370.4$ and $ASS_0 = 5$.

The computed control limits (g, h) of the OSPRT chart for each pair of (k, γ), as well as the resulting (ARL, SDRL) values under the Normal distribution, are presented in Table 1. The performance metrics are evaluated for $\delta \in \{0.0, 0.5, 1.0, 1.5, 2.0\}$ and $\eta \in \{1.0, 1.5, 2.0\}$. It should be noted that all the results have been computed from Equations (10) and (11) using $L = 200$, and their accuracies have been checked through Monte Carlo simulation. To provide a numeric example, when $k = 0.1$ and $\gamma = 5.0$ are selected, the computed control limits are (g, h) = (–17.921, 4.501). Under the Normal distribution, the ARL_1 and the out-of-control SDRL ($SDRL_1$) values are read off as 1.54 and 0.92, respectively, when (δ, η) = (1.0, 2.0). From the results tabulated in Table 1, it is noticed that generally, the (ARL_1, $SDRL_1$) values decrease as the magnitude of the shift size increases. For example, when $k = 0.1$ and $\gamma = 5.0$ are selected, the (ARL_1, $SDRL_1$) values are found to decrease as η increases from 1.0 through 2.0 for each value of δ. However, when the mean shift size is large, i.e., $\delta \geq 1.5$, a different

pattern has been observed. Particularly, it is found that when δ = 2.0, the (ARL_1, $SDRL_1$) values for the combinations $(k, \gamma) \in \{(0.1, 2.0), (0.5, 2.5)\}$ increase slightly as η increases. This phenomenon has been explained by Teoh et al. [10] in their article, citing multiple joint monitoring control schemes that have reported the same unusual trend. However, it is worth noting that in practice, this phenomenon is far less concerning, as the (ARL_1, $SDRL_1$) values are already adequately close to their minimum values (i.e., one and zero).

Equipped with the charting parameters in Table 1, we can now proceed to evaluate the performances of the OSPRT chart designed for the Normal distribution, in the case where the underlying data follow the Weibull distribution. The performances of the OSPRT chart are evaluated under two different cases, i.e., (i) when the data have zero skewness, and (ii) when the data have positive skewness. In case (ii), we select three different values of θ, i.e., $\theta \in \{1.0, 2.0, 3.0\}$, to represent low, moderate, and high levels of skewness of the Weibull distribution. To calculate the ARL and SDRL values of the OSPRT chart, we simulate measurements from the Weibull distribution with various degrees of skewness. The shape parameter β is determined by substituting the appropriate values of θ in Equation (16) and solving the equation via some numerical techniques (e.g., the secant method). For instance, if we wish to determine the value of β that corresponds to a skewness level of 0.0, we substitute θ = 0.0 in Equation (16) and solve the equation. The resulting value of β is obtained as 3.6023 (to an accuracy of 0.0001). Table 2 shows the (ARL, SDRL) values of the OSPRT chart designed for the Normal

Table 1 *Charting parameters (k, γ, g, h) of the OSPRT chart designed for the Normal distribution, together with the (ARL, SDRL) values for δ ∈{0.0, 0.5, 1.0, 1.5, 2.0} and η ∈{1.0, 1.5, 2.0}, when the underlying data follow the Normal distribution, ARL_0 = 370.4, and ASS_0 = 5*

(k, γ)		(0.1, 2.0)	(0.1, 5.0)	(0.5, 2.5)	(0.5, 6.0)
(g, h)		(−4.121, 11.270)	(−17.921, 4.501)	(−5.217, 13.036)	(−21.331, 5.287)
δ	η	(ARL, SDRL)	(ARL, SDRL)	(ARL, SDRL)	(ARL, SDRL)
0.0	1.0	(370.40, 369.90)	(370.40, 369.90)	(370.40, 369.90)	(370.40, 369.90)
	1.5	(2.71, 2.15)	(10.86, 10.35)	(3.77, 3.23)	(14.29, 13.78)
	2.0	(1.26, 0.58)	(2.33, 1.77)	(1.40, 0.75)	(3.01, 2.46)
0.5	1.0	(38.17, 37.66)	(104.58, 104.08)	(13.43, 12.92)	(70.55, 70.04)
	1.5	(1.95, 1.36)	(6.92, 6.40)	(1.86, 1.27)	(6.47, 5.95)
	2.0	(1.21, 0.51)	(2.01, 1.42)	(1.25, 0.56)	(2.16, 1.58)
1.0	1.0	(2.53, 1.96)	(21.09, 20.58)	(1.45, 0.81)	(13.39, 12.88)
	1.5	(1.34, 0.67)	(3.27, 2.72)	(1.23, 0.53)	(2.75, 2.19)
	2.0	(1.13, 0.39)	(1.54, 0.92)	(1.13, 0.38)	(1.51, 0.88)
1.5	1.0	(1.10, 0.34)	(4.17, 3.64)	(1.03, 0.17)	(2.55, 1.99)
	1.5	(1.10, 0.33)	(1.63, 1.02)	(1.06, 0.25)	(1.40, 0.75)
	2.0	(1.07, 0.27)	(1.22, 0.52)	(1.06, 0.24)	(1.18, 0.46)
2.0	1.0	(1.01, 0.09)	(1.21, 0.51)	(1.00, 0.04)	(1.05, 0.23)
	1.5	(1.03, 0.16)	(1.12, 0.36)	(1.01, 0.11)	(1.06, 0.25)
	2.0	(1.03, 0.18)	(1.07, 0.28)	(1.02, 0.15)	(1.05, 0.23)

distribution, in the case where the data follow the Weibull distribution with zero skewness. The performance metrics are evaluated for $\delta \in \{0.0, 0.5, 1.0, 1.5, 2.0\}$ and $\eta \in \{1.0, 1.5, 2.0\}$. All the values are computed using Monte Carlo simulation with 100,000 simulation runs to ensure the reliability of the results. As a numeric example, the (ARL_0, $SDRL_0$) values of the OSPRT chart with (k, γ) = (0.1, 5.0) are equal to (1135.97, 1135.47) (see Table 2). To compute the ARL_1 and $SDRL_1$ values for each pair of (δ, η), we first simulate independent observations $X_{i,j}$ from the in-control Weibull distribution with shape parameter β = 3.6023 and scale parameter 1. We then apply the transformation $Y_{i,j} = \eta X_{i,j} + \delta\sigma_0 - (\eta - 1)\mu_0$ to obtain the out-of-control data values. It is easy to show that, if $E[X_{i,j}] = \mu_0$ and $Var(X_{i,j}) = \sigma_0$, then $E[Y_{i,j}] = \mu_0 + \delta\sigma_0$ and $Var(Y_{i,j}) = \eta\sigma_0$.

From Table 2, it is observed that the ARL_0 and $SDRL_0$ values of the OSPRT chart increase tremendously when the data assume a symmetric Weibull distribution. In particular, for the combinations $(k, \gamma) \in \{(0.5, 2.5), (0.5, 6.0)\}$, the ($ARL_0$, $SDRL_0$) values are almost twice as large as the nominal values (370.40, 369.90), whereas for the combinations $(k, \gamma) \in \{(0.1, 2.0), (0.1, 5.0)\}$, the ($ARL_0$, $SDRL_0$) values are almost three times as large as (370.40, 369.90). This finding is rather surprising, since we expect the OSPRT chart to have similar performances to that in table 1, when the Weibull distribution with zero skewness is assumed. Although the results have gone against our anticipation, we are not too concerned about the increase in the ARL_0 value, since an increased ARL_0 indicates that false alarms have decreased on average. On the other hand, it is generally found

Table 2 *The (ARL, SDRL) values of the OSPRT chart designed for the normal distribution, when the underlying data follow the Weibull distribution with zero skewness*

Int. Journal of Integrated Engineering Vol. 16 No. 5 (2024) p. 201-213

(k, γ)		(0.1, 2.0)	(0.1, 5.0)	(0.5, 2.5)	(0.5, 6.0)
(g, h)		(−4.121, 11.270)	(−17.921, 4.501)	(−5.217, 13.036)	(−21.331, 5.287)
δ	η	(ARL, SDRL)	(ARL, SDRL)	(ARL, SDRL)	(ARL, SDRL)
0.0	1.0	(1169.55, 1169.05)	(1135.97, 1135.47)	(752.31, 751.81)	(691.07, 690.57)
	1.5	(2.55, 1.98)	(13.14, 12.63)	(3.69, 3.15)	(17.42, 16.91)
	2.0	(1.23, 0.53)	(2.29, 1.72)	(1.35, 0.68)	(3.04, 2.49)
0.5	1.0	(48.36, 47.86)	(150.67, 150.17)	(14.38, 13.87)	(92.04, 91.53)
	1.5	(1.86, 1.26)	(7.65, 7.13)	(1.81, 1.21)	(6.86, 6.34)
	2.0	(1.18, 0.47)	(1.97, 1.38)	(1.22, 0.52)	(2.13, 1.56)
1.0	1.0	(2.48, 1.92)	(23.78, 23.28)	(1.45, 0.81)	(14.38, 13.87)
	1.5	(1.31, 0.64)	(3.30, 2.75)	(1.23, 0.53)	(2.73, 2.18)
	2.0	(1.12, 0.36)	(1.51, 0.88)	(1.12, 0.36)	(1.49, 0.86)
1.5	1.0	(1.11, 0.35)	(4.20, 3.66)	(1.03, 0.18)	(2.53, 1.97)
	1.5	(1.10, 0.33)	(1.61, 0.99)	(1.06, 0.26)	(1.39, 0.74)
	2.0	(1.06, 0.26)	(1.21, 0.50)	(1.06, 0.24)	(1.17, 0.45)
2.0	1.0	(1.01, 0.09)	(1.21, 0.50)	(1.00, 0.04)	(1.05, 0.23)
	1.5	(1.03, 0.17)	(1.11, 0.36)	(1.01, 0.12)	(1.06, 0.25)
	2.0	(1.03, 0.18)	(1.07, 0.27)	(1.02, 0.16)	(1.05, 0.23)

that the out-of-control performances of the OSPRT chart do not get affected much by the increased ARL_0 value. In particular, the (ARL_1, $SDRL_1$) values of the OSPRT chart in Table 2 are reasonably close to those in Table 1 for almost all the shift sizes, except for a few instances, i.e., $(\delta, \eta) \in \{(0.0, 1.5), (0.5, 1.0)\}$. Generally, the performances of the OSPRT chart designed for the Normal distribution are said to be quite satisfactory when the underlying data follow a symmetric Weibull distribution.

Table 3 shows the (ARL, SDRL) values of the OSPRT chart designed for the Normal distribution, in the case where the data follow the Weibull distribution with $\theta \in \{1.0, 2.0, 3.0\}$, for $\delta \in \{0.0, 0.5, 1.0, 1.5, 2.0\}$ and $\eta \in \{1.0, 1.5, 2.0\}$. As a numeric example, when $\theta = 3.0$ (i.e., $\beta = 0.7686$), the (ARL_0, $SDRL_0$) values of the OSPRT chart with $(k, \gamma) = (0.5, 6.0)$ are equal to (17.84, 17.34) (see Table 3). From Table 3, one notices that the in-control performances of the OSPRT chart designed for the Normal distribution deteriorate for all levels of skewness of the Weibull distribution. When the skewness level is low (i.e., $\theta = 1.0$), the ARL_0 and $SDRL_0$ values diminish to only around 40 to 60 (see Table 3), as compared to the original values of 370.4 and 369.9 observed in Table 1. As the skewness level increases further, the ARL_0 and $SDRL_0$ values are found to drop further, levelling off at probably around $\theta = 3.0$. The tremendous fall in the ARL_0 values is undoubtedly a red flag in SQC applications, since low ARL_0 values indicate that there are many false alarms on average. Although the perceived fall in the $SDRL_0$ values may indicate that the in-control performances have become more consistent, practitioners still face the predicament of constant disturbance from the massive number of false signals emitted by the system. Hence, some remedial strategies must be proposed to correct the design of the OSPRT chart under skewed data distributions. In the out-of-control situation, it is found that generally, the (ARL_1, $SDRL_1$) values decrease because of an increased skewness. For instance, when $(k, \gamma) = (0.5, 2.5)$ and $\theta = 1.0$, the (ARL_1, $SDRL_1$) values at $(\delta, \eta) = (0.5, 1.0)$ are found to be (8.36, 7.84) (see Table 3), as compared to the original values of (13.43, 12.92) (see Table 1). However, we have observed the exact opposite in most of the cases with large process mean shift sizes (i.e., $\delta \geq 1.5$). For instance, when $(k, \gamma) = (0.1, 2.0)$ and $\theta = 1.0$, the (ARL_1, $SDRL_1$) values at $(\delta, \eta) = (1.5, 1.0)$ are equal to (1.20, 0.49) (see Table 3), as compared to the original values of (1.10, 0.34) (see Table 1). As the out-of-control performances are inconsistent across different shift sizes and the choices of (k, γ), practitioners have a stronger urge to pursue a new design for the OSPRT chart under the Weibull distribution, considering that the in-control performances are also highly unsatisfactory.

3.2 The OSPRT Chart with Skewness-corrected Control Limits Under The Weibull Distribution

To restore the in-control performances of the OSPRT chart under the Weibull distribution, we suggest a new method for re-computing the control limits of the OSPRT chart. This method is known as skewness correction. As the ARL_0 and ASS_0 values have deteriorated under the influence of the Weibull distribution, it is necessary to correct the control limits of the OSPRT chart to ensure that the initial design specifications are met. It should be noted that different degrees of skewness can have different impacts on the performance metrics of the OSPRT chart (e.g., a larger skewness likely leads to a smaller ARL_0). Therefore, the method is set out to adjust the control limits of the OSPRT chart according to a specific value of θ. Note that the method does not apply when the Weibull distribution assumes zero skewness, since the in-control performance of the SPRT chart is not

adversely affected under a symmetric Weibull distribution. The strategy for implementing skewness correction on the OSPRT chart is detailed as follows:

1) Input the design parameters of the OSPRT chart, i.e., the reference parameters (k and γ) and the in-control specifications (τ and n).
2) Initiate the corrected limits g' and h' equal to the values of g and h obtained from the OSPRT chart designed for the Normal distribution.
3) Adjust the values of g' and h' to satisfy the constraints $ASS_0 = n$ and $ARL_0 = \tau$, respectively. According to Deore et al. [12], the value of g' is more sensitive to changes in the ASS_0, whereas the value of h' is more sensitive to changes in the ARL_0. An efficient algorithm can be written based on this observation to speed up the search process. The algorithm is terminated once the values of g' and h' have converged.

Table 4 displays the skewness-corrected control limits (g', h') on the top row of each subsection, and the (ARL, SDRL) values of the OSPRT chart for $\delta \in \{0.0, 0.5, 1.0, 1.5, 2.0\}$ and $\eta \in \{1.0, 1.5, 2.0\}$ in the subsequent rows. As a numeric example, when (k, γ) = (0.1, 2.0) and θ = 3.0, the skewness-corrected control limits are calculated as (g', h') = (−4.238, 78.008). The resulting (ARL_1, $SDRL_1$) values evaluated at (δ, η) = (1.5, 1.0) are read off as (1.25, 0.56). From Table 4, it is observed that, as the skewness level increases, the adjusted upper control limit h' increases. This observation can be explained by the fact that the decreased ARL_0 value needs to be compensated by a larger upper control limit h'. When h' is elevated, the control statistic of the OSPRT chart has a smaller chance of falling in the out-of-control region, thus lowering the false alarm probability. As the false alarm probability decreases, the ARL_0 value can be successfully restored to the recommended level τ. Referring to the adjusted lower control limit g', one observes very minute changes induced by the algorithm as the level of

Table 3 *The (ARL, SDRL) values of the OSPRT chart designed for the Normal distribution, when the underlying data follow the Weibull distribution with skewness $\theta \in \{1.0, 2.0, 3.0\}$*

		(k, γ)		(0.1, 2.0)	(0.1, 5.0)	(0.5, 2.5)	(0.5, 6.0)
		(g, h)		(−4.121, 11.270)	(−17.921, 4.501)	(−5.217, 13.036)	(−21.331, 5.287)
β	θ	δ	η	(ARL, SDRL)	(ARL, SDRL)	(ARL, SDRL)	(ARL, SDRL)
1.5639	1.0	0.0	1.0	(51.34, 50.83)	(57.74, 57.24)	(40.47, 39.97)	(48.80, 48.30)
			1.5	(3.38, 2.84)	(8.03, 7.51)	(4.48, 3.95)	(7.87, 7.35)
			2.0	(1.31, 0.63)	(2.81, 2.25)	(1.75, 1.14)	(3.18, 2.63)
		0.5	1.0	(14.33, 13.82)	(23.83, 23.33)	(8.36, 7.84)	(19.22, 18.72)
			1.5	(2.73, 2.17)	(5.01, 4.48)	(2.57, 2.01)	(4.59, 4.06)
			2.0	(1.42, 0.77)	(2.36, 1.79)	(1.62, 1.00)	(2.39, 1.82)
		1.0	1.0	(3.12, 2.58)	(9.28, 8.76)	(1.78, 1.18)	(7.06, 6.54)
			1.5	(1.80, 1.20)	(3.00, 2.45)	(1.54, 0.91)	(2.63, 2.07)
			2.0	(1.37, 0.71)	(1.85, 1.26)	(1.38, 0.72)	(1.78, 1.18)
		1.5	1.0	(1.20, 0.49)	(3.35, 2.80)	(1.04, 0.20)	(2.39, 1.82)
			1.5	(1.27, 0.58)	(1.82, 1.22)	(1.14, 0.39)	(1.57, 0.95)
			2.0	(1.23, 0.53)	(1.45, 0.81)	(1.18, 0.46)	(1.37, 0.71)
		2.0	1.0	(1.00, 0.06)	(1.31, 0.64)	(1.00, 0.00)	(1.08, 0.30)
			1.5	(1.06, 0.25)	(1.23, 0.53)	(1.02, 0.13)	(1.12, 0.36)
			2.0	(1.10, 0.34)	(1.19, 0.48)	(1.06, 0.25)	(1.13, 0.38)
1.0000	2.0	0.0	1.0	(24.04, 23.53)	(24.40, 23.89)	(20.80, 20.29)	(22.37, 21.87)
			1.5	(4.88, 4.36)	(6.65, 6.13)	(5.54, 5.01)	(6.67, 6.15)
			2.0	(1.85, 1.25)	(3.29, 2.75)	(2.75, 2.19)	(3.53, 2.98)
		0.5	1.0	(11.36, 10.85)	(13.98, 13.47)	(7.94, 7.42)	(12.14, 11.63)
			1.5	(3.86, 3.32)	(4.86, 4.33)	(3.38, 2.84)	(4.52, 3.99)
			2.0	(2.17, 1.60)	(2.81, 2.26)	(2.33, 1.76)	(2.80, 2.25)
		1.0	1.0	(3.84, 3.30)	(7.32, 6.80)	(2.13, 1.55)	(5.96, 5.44)
			1.5	(2.39, 1.82)	(3.28, 2.73)	(1.89, 1.30)	(2.90, 2.35)
			2.0	(1.90, 1.30)	(2.26, 1.69)	(1.73, 1.13)	(2.12, 1.54)
		1.5	1.0	(1.25, 0.56)	(3.40, 2.85)	(1.02, 0.14)	(2.54, 1.98)
			1.5	(1.43, 0.79)	(2.10, 1.52)	(1.17, 0.44)	(1.79, 1.19)
			2.0	(1.46, 0.82)	(1.73, 1.12)	(1.29, 0.61)	(1.58, 0.96)
		2.0	1.0	(1.00, 0.00)	(1.43, 0.79)	(1.00, 0.00)	(1.12, 0.36)
			1.5	(1.04, 0.21)	(1.35, 0.69)	(1.00, 0.04)	(1.18, 0.45)
			2.0	(1.15, 0.42)	(1.33, 0.66)	(1.06, 0.24)	(1.21, 0.51)
0.7686	3.0	0.0	1.0	(20.27, 19.76)	(19.03, 18.52)	(18.12, 17.61)	(17.84, 17.34)

Int. Journal of Integrated Engineering Vol. 16 No. 5 (2024) p. 201-213

			1.5	(6.34, 5.82)	(6.83, 6.31)	(6.52, 6.00)	(6.84, 6.32)
			2.0	(2.88, 2.33)	(3.84, 3.31)	(3.80, 3.26)	(4.07, 3.54)
		0.5	1.0	(11.52, 11.01)	(12.32, 11.81)	(8.57, 8.05)	(10.95, 10.44)
			1.5	(4.82, 4.29)	(5.26, 4.74)	(4.15, 3.62)	(4.90, 4.38)
			2.0	(3.07, 2.52)	(3.34, 2.80)	(2.96, 2.40)	(3.26, 2.71)
		1.0	1.0	(4.58, 4.05)	(7.23, 6.71)	(2.44, 1.87)	(6.00, 5.48)
			1.5	(2.95, 2.40)	(3.70, 3.16)	(2.21, 1.64)	(3.27, 2.72)
			2.0	(2.37, 1.81)	(2.66, 2.10)	(2.05, 1.47)	(2.47, 1.90)
		1.5	1.0	(1.26, 0.57)	(3.68, 3.14)	(1.00, 0.07)	(2.79, 2.23)
			1.5	(1.54, 0.92)	(2.40, 1.83)	(1.15, 0.41)	(2.02, 1.43)
			2.0	(1.65, 1.03)	(2.00, 1.41)	(1.35, 0.68)	(1.78, 1.18)
		2.0	1.0	(1.00, 0.00)	(1.55, 0.92)	(1.00, 0.00)	(1.14, 0.40)
			1.5	(1.01, 0.11)	(1.46, 0.82)	(1.00, 0.00)	(1.22, 0.52)
			2.0	(1.14, 0.39)	(1.44, 0.80)	(1.02, 0.14)	(1.28, 0.59)

skewness increases. It might be reasonable to say that an increased skewness does not impose much impact on the ASS_0 performance of the OSPRT chart.

From the (ARL, SDRL) values in Table 4, it is evident that the skewness correction method has effectively restored the in-control performance of the OSPRT chart. All the (ARL_0, $SDRL_0$) values are found to be approximately equal to (370.4, 369.9) following the adjustment made to the control limits of the OSPRT chart. However, the out-of-control performances of the skewness-corrected OSPRT chart become worse as compared to the uncorrected OSPRT chart. For instance, when (k, γ) = (0.5, 2.5), (δ, η) = (0.5, 2.0), and θ = 2.0, the skewness-corrected OSPRT chart produces (ARL_1, $SDRL_1$) = (2.61, 2.05) (see Table 4), which are slightly higher

Table 4 *Adjusted control limits (g', h') of the OSPRT chart designed for the Weibull distribution with skewness $\theta \in \{1.0, 2.0, 3.0\}$, together with the (ARL, SDRL) values for $\delta \in \{0.0, 0.5, 1.0, 1.5, 2.0\}$ and $\eta \in \{1.0, 1.5, 2.0\}$, when ARL_0 = 370.4 and ASS_0 = 5*

		(k, γ)		(0.1, 2.0)	(0.1, 5.0)	(0.5, 2.5)	(0.5, 6.0)
				(g', h')	(g', h')	(g', h')	(g', h')
β	θ	δ	η	(ARL, SDRL)	(ARL, SDRL)	(ARL, SDRL)	(ARL, SDRL)
				(−4.179, 23.028)	(−17.940, 13.231)	(−5.128, 28.058)	(−21.481, 15.801)
1.5639	1.0	0.0	1.0	(370.40, 369.90)	(370.40, 369.90)	(370.40, 369.90)	(370.40, 369.90)
			1.5	(4.25, 3.72)	(18.94, 18.43)	(7.03, 6.51)	(20.10, 19.60)
			2.0	(1.31, 0.63)	(4.09, 3.55)	(1.81, 1.22)	(4.95, 4.42)
		0.5	1.0	(52.91, 52.41)	(125.18, 124.68)	(25.98, 25.48)	(113.04, 112.54)
			1.5	(3.12, 2.57)	(10.19, 9.68)	(3.03, 2.48)	(9.71, 9.19)
			2.0	(1.42, 0.77)	(3.18, 2.64)	(1.66, 1.04)	(3.33, 2.79)
		1.0	1.0	(4.04, 3.50)	(35.79, 35.28)	(1.90, 1.31)	(27.54, 27.03)
			1.5	(1.85, 1.25)	(5.00, 4.48)	(1.58, 0.96)	(4.32, 3.79)
			2.0	(1.36, 0.71)	(2.28, 1.71)	(1.39, 0.74)	(2.19, 1.62)
		1.5	1.0	(1.20, 0.49)	(7.68, 7.16)	(1.04, 0.20)	(4.61, 4.08)
			1.5	(1.27, 0.58)	(2.38, 1.81)	(1.14, 0.40)	(1.94, 1.35)
			2.0	(1.23, 0.53)	(1.63, 1.01)	(1.18, 0.46)	(1.51, 0.87)
		2.0	1.0	(1.00, 0.06)	(1.52, 0.89)	(1.00, 0.00)	(1.12, 0.36)
			1.5	(1.06, 0.24)	(1.32, 0.65)	(1.02, 0.13)	(1.15, 0.42)
			2.0	(1.10, 0.33)	(1.24, 0.55)	(1.06, 0.26)	(1.16, 0.43)
				(−4.263, 48.196)	(−18.249, 33.915)	(−4.978, 54.862)	(−21.598, 37.795)
1.0000	2.0	0.0	1.0	(370.40, 369.90)	(370.40, 369.90)	(370.40, 369.90)	(370.40, 369.90)
			1.5	(8.66, 8.15)	(29.25, 28.74)	(13.21, 12.70)	(31.14, 30.64)
			2.0	(1.86, 1.27)	(7.20, 6.68)	(3.30, 2.76)	(8.36, 7.84)
		0.5	1.0	(95.50, 95.00)	(189.39, 188.89)	(51.31, 50.81)	(171.98, 171.48)
			1.5	(5.70, 5.18)	(18.52, 18.01)	(5.07, 4.55)	(17.49, 16.98)
			2.0	(2.25, 1.68)	(5.61, 5.09)	(2.61, 2.05)	(5.78, 5.26)
		1.0	1.0	(6.80, 6.28)	(76.70, 76.20)	(2.45, 1.89)	(59.39, 58.89)
			1.5	(2.64, 2.08)	(9.69, 9.18)	(2.04, 1.45)	(8.12, 7.61)
			2.0	(1.93, 1.34)	(3.86, 3.32)	(1.81, 1.21)	(3.57, 3.03)
		1.5	1.0	(1.24, 0.54)	(19.13, 18.62)	(1.02, 0.15)	(10.27, 9.76)
			1.5	(1.42, 0.78)	(4.11, 3.58)	(1.18, 0.47)	(3.04, 2.49)
			2.0	(1.46, 0.82)	(2.40, 1.83)	(1.31, 0.64)	(2.08, 1.50)

		2.0	1.0	(1.00, 0.00)	(2.08, 1.50)	(1.00, 0.00)	(1.18, 0.46)
			1.5	(1.04, 0.20)	(1.63, 1.01)	(1.00, 0.05)	(1.27, 0.58)
			2.0	(1.14, 0.41)	(1.50, 0.86)	(1.06, 0.26)	(1.30, 0.63)
				(–4.238, 78.008)	(–18.576, 60.018)	(–4.980, 85.840)	(–21.757, 65.142)
0.7686	3.0	0.0	1.0	(370.40, 369.90)	(370.40, 369.90)	(370.40, 369.90)	(370.40, 369.90)
			1.5	(15.13, 14.62)	(40.42, 39.91)	(20.43, 19.92)	(43.79, 43.28)
			2.0	(3.20, 2.65)	(11.13, 10.62)	(5.40, 4.87)	(12.88, 12.37)
		0.5	1.0	(134.11, 133.61)	(229.38, 228.87)	(77.41, 76.91)	(210.90, 210.40)
			1.5	(9.07, 8.55)	(28.53, 28.03)	(7.62, 7.10)	(27.07, 26.56)
			2.0	(3.55, 3.01)	(8.82, 8.30)	(3.68, 3.14)	(9.05, 8.54)
		1.0	1.0	(10.33, 9.82)	(114.07, 113.57)	(2.96, 2.41)	(91.18, 90.68)
			1.5	(3.57, 3.03)	(15.85, 15.34)	(2.47, 1.91)	(13.25, 12.74)
			2.0	(2.55, 1.99)	(5.96, 5.44)	(2.23, 1.65)	(5.42, 4.89)
		1.5	1.0	(1.25, 0.56)	(34.65, 34.15)	(1.01, 0.07)	(18.50, 17.99)
			1.5	(1.54, 0.91)	(6.45, 5.93)	(1.16, 0.44)	(4.47, 3.94)
			2.0	(1.65, 1.04)	(3.37, 2.82)	(1.37, 0.72)	(2.77, 2.21)
		2.0	1.0	(1.00, 0.00)	(2.69, 2.14)	(1.00, 0.00)	(1.22, 0.52)
			1.5	(1.01, 0.10)	(1.93, 1.34)	(1.00, 0.00)	(1.35, 0.69)
			2.0	(1.13, 0.38)	(1.75, 1.14)	(1.02, 0.15)	(1.42, 0.77)

than those of the uncorrected OSPRT chart (= (2.33, 1.76)) (see Table 3). While the degraded out-of-control performance may be undesirable, it is justified on the grounds of an increased upper control limit. As h' is inflated to bring the ARL_0 value back to 370.4, it is expected that the (ARL_1, $SDRL_1$) values will also increase. Meanwhile, it is perhaps quite relieving that the out-of-control performances do not deteriorate to an intolerable degree. Most of the most impactful deteriorations are found to occur at relatively small shift sizes (i.e., $\delta = 0.5$), whereas the majority of the (ARL_1, $SDRL_1$) values evaluated at moderate and large shift sizes (i.e., $\delta \geq 1.5$) are almost unaffected by skewness correction. For instance, when $\theta = 1.0$ and (δ, η) = (0.5, 1.0) (i.e., small process means shift), the (ARL_1, $SDRL_1$) values for the skewness-corrected OSPRT chart range from 26 to around 125 (see Table 4). These values are almost 4 or 5 times greater than those of the uncorrected OSPRT chart, which range from 8 to around 24 (see Table 3). However, for moderate and large shift sizes, the out-of-control performances are almost the same for both the corrected and uncorrected OSPRT charts.

4. An Illustration of The Proposed OSPRT Chart

This section aims to provide an illustration of the proposed OSPRT chart for monitoring Weibull distributed processes. We have chosen an application in the materials industry, i.e., to monitor the compressive strength of carbon fibers. Carbon fibers are extensively used in the aerospace and automotive sectors for manufacturing lightweight and high-strength components. These include aircraft components such as wings, fuselage sections, and interior structures, as well as components of automobiles such as body panels, chassis parts etc. The production of carbon fibers involves several processes, and various inadequacies in the production stages can affect the compressive strength of the final product. For example, an ill-controlled heating temperature in the carbonization process likely leads to an incomplete conversion of the precursor material to carbon, thus leading to a reduced compressive strength. Other factors such as improper graphitization conditions, misalignment, or irregularities in the fiber orientation, may also result in unstable compressive strength values. While a reduction in the compressive strength is often the sign of poor quality, it is not unusual to observe an increase in the compressive strength values due to erroneous measurements made by quality inspectors, which creates a false sign of an improved fibrous quality. Hence, it is necessary to detect changes in both directions of the process mean, as well as an increasing shift in the process variance.

Suppose that the compressive strength of a certain type of high modulus carbon fiber is found to follow the Weibull distribution with shape parameter $\beta = 0.7686$ and scale parameter $\lambda = 1$. The mean compressive strength is calculated as 1.167 gigapascal (GPa), whereas the standard deviation of the compressive strength is calculated as 1.537 GPa. We will select the charting parameters of the OSPRT chart designed for the Weibull distribution corresponding to $\theta = 3.0$ from Table 4. For the purpose of illustration, we select the combination (k, γ) = (0.5, 2.5) in our application, and the adjusted control limits are given as $g' = -4.980$ and $h' = 85.840$. The upper- and lower-sided control statistics, $T_{i,j}^{+}$ and $T_{i,j}^{-}$, of the OSPRT chart are then calculated using the formulae

$$T_{i,j}^{+} = \sum_{j'=1}^{j} \left[\left(\frac{Y_{i,j'} - 1.167}{1.537} + 0.5 \right)^2 - 2.5 \right] \tag{17}$$

Int. Journal of Integrated Engineering Vol. 16 No. 5 (2024) p. 201-213

and

$$T_{i,j}^{-} = \sum_{j'=1}^{j}\left[\left(\frac{Y_{i,j'}-1.167}{1.537}-0.5\right)^2-2.5\right], \tag{18}$$

respectively.

Figure 1 displays the Phase-II application of the proposed OSPRT chart for monitoring compressive strength values generated using simulation. The dashed line represents the path of $T_{i,j}^{+}$, whereas the solid line represents the path of $T_{i,j}^{-}$. Assume that, during the inspection process, the loading axis of the testing machine is misaligned, causing the distribution of the compressive strength measurements to shift by δ = 1.0 and η = 1.2. In other words, the mean and standard deviation of the compressive strength values shift to 2.705 GPa and 1.845 GPa, respectively. We observe, from Figure 5, that the joint shift is detected within four samples. In the first three samples, the process is declared as in-control as both $T_{i,j}^{+}$ and $T_{i,j}^{-}$ fall below the lower control limit g'. In the fourth sample, the upper-sided control statistic $T_{i,j}^{+}$ goes above the upper control limit h' after 10 observations are acquired, indicating that there is a fault in either the production or measurement stage. The quality engineer quickly finds out that the testing machine was inappropriately aligned, and subsequently proceed with corrective actions to restore the status of the process.

5. Conclusions

In this paper, we conduct a thorough analysis of the performances of the OSPRT chart designed for the Normal distribution, when the underlying data assumes a Weibull distribution. The paper provides an overview of how the OSPRT scheme works, how different levels of skewness may affect the performances of the OSPRT chart, followed by the introduction of a novel method for redesigning the OSPRT chart under the Weibull distribution. In practice, the Weibull distribution is found to be useful in modelling a wide variety of variables, such as failure times in life testing, the mechanical strength of plant fibers, wind velocity, etc. Therefore, it is selected as the main premise of our research study.

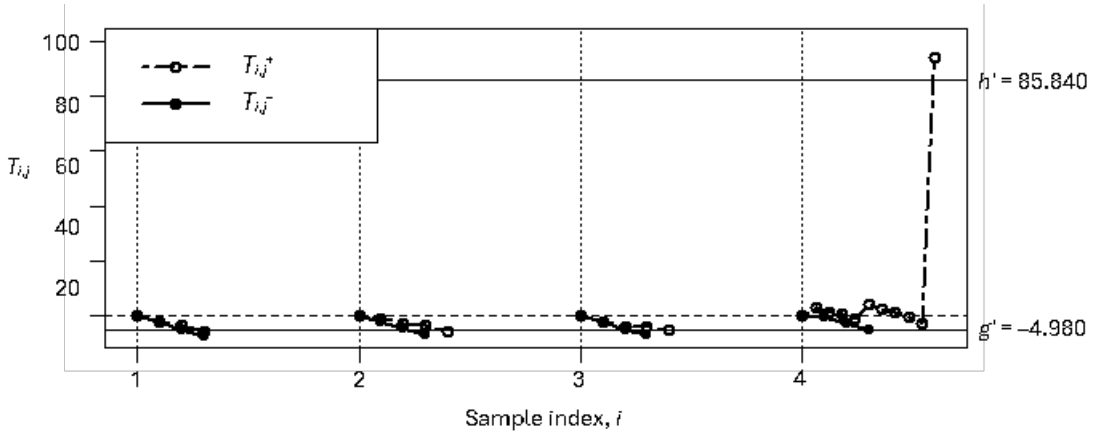

Fig. 1 *The OSPRT chart with skewness-adjusted control limits for monitoring the compressive strength of carbon fibers*

Based on the results, we discover that the OSPRT chart designed for the Normal distribution performs undesirably in all levels of skewness of the Weibull distribution. It is found that the ARL_0 value decreases substantially even when there exists a small skewness in the data, i.e., θ = 1.0. The out-of-control performances of the OSPRT chart are also quite inconsistent across various shift sizes and choices of (k, γ), necessitating the development of a new correction strategy for the OSPRT chart. To address the issue, we propose a new skewness correction design for the OSPRT chart under the Weibull distribution. In our new design, the control limits of the OSPRT chart are re-adjusted by ensuring that the ARL_0 and ASS_0 values satisfy the initial settings. By conducting simulation studies, we show that the OSPRT chart with skewness-corrected control limits successfully restores the (ARL_0, $SDRL_0$) values back to their recommended levels, thus eliminating the concerns about reduced productivity due to excessive false alarms. It is also found that the out-of-control performances of the OSPRT chart deteriorate slightly because of the skewness correction design. However, the degradation is acceptable due to the general trade-off between in-control and out-of-control performances of control charts.

Future research may explore a new OSPRT scheme designed specifically for the Weibull distribution, i.e., through deriving a new control statistic for the OSPRT scheme based on the likelihood function of the Weibull distribution. Alternatively, researchers may consider developing optimal designs for the OSPRT chart based on

the skewness correction method, which is hoped to further improve the out-of-control performance of the OSPRT chart.

Acknowledgement

This work was supported by the Ministry of Higher Education (MOHE) Malaysia and Heriot-Watt University Malaysia under the Fundamental Research Grant Scheme (FRGS), no. FRGS/1/2021/STG06/HWUM/02/1.

Conflict of Interest

Authors declare that there is no conflict of interest regarding the publication of the paper.

Author Contribution

The authors confirm contribution to the paper as follows: ***study conception and design:*** *J.W. Teoh, W.L. Teoh;* ***data collection:*** *J.W. Teoh, W.L. Teoh;* ***analysis and interpretation of results:*** *J.W. Teoh, Z.L. Chong;* ***draft manuscript preparation:*** *J.W. Teoh, W.L. Teoh, Z.L. Chong, X.Y. Chew, S.Y. Teh. All authors reviewed the results and approved the final version of the manuscript.*

References

[1] Montgomery, D. C. (2013). *Introduction to Statistical Quality Control*. 7th ed. New York: John Wiley & Sons.
[2] Kasmin, A., Masood, I., Abdul Rahman, N., Abdul Kadir, A. H., & Abdol Rahman, M. N. (2021). Control chart pattern recognition using small window size for identifying bivariate process mean shifts. *International Journal of Integrated Engineering*, *13*(2), 208-213. https://doi.org/10.30880/ijie.2021.13.02.024
[3] Kasmin, A., Masood, I., Abdul Rahman, N., Abdul Kadir, A. H., & Abdol Rahman, M. N. (2021). Identifying unnatural variation in precision rotational part manufacturing. *International Journal of Integrated Engineering*, *13*(2), 189-195. https://doi.org/10.30880/ijie.2021.13.02.021
[4] You, H. W., Chong, Z. L., Teoh, W. L., Khoo, M. B. C., & Yeong, W. C. (2023). An expected average run length (EARL) performance comparison of the SSGR and EWMA control charts. *International Journal of Integrated Engineering*, *15*(5), 35-40. https://doi.org/10.30880/ijie.2023.15.05.005
[5] Mou, Z., Chiang, J. Y., Bai, Y., & Chen, S. (2023). A self-starting non-restarting CUSUM chart for monitoring Poisson count data with time-varying sample sizes. *Computers & Industrial Engineering*, *184*(10), Article 109599. https://doi.org/10.1016/j.cie.2023.109599
[6] Mim, F. N., Khoo, M. B. C., Saha, S., & Haq, A. (2022). New run sum *t* charts with variable sampling intervals for process mean. *Communications in Statistics-Simulation and Computation*, *51*(9), 5350-5372. https://doi.org/10.1080/03610918.2020.1770285
[7] Haq, A., & Razzaq, F. (2020). Maximum weighted adaptive CUSUM charts for simultaneous monitoring of process mean and variance. *Journal of Statistical Computation and Simulation*, *90*(16), 2949-2974. https://doi.org/10.1080/00949655.2020.1793154
[8] Arif, F., Noor-ul-Amin, M., & Hanif, M. (2022). Joint monitoring of mean and variance under double ranked set sampling using likelihood ratio test statistic. *Communications in Statistics-Theory and Methods*, *51*(17), 6032-6048. https://doi.org/10.1080/03610926.2020.1851721
[9] Chatterjee, K., Koukouvinos, C., & Lappa, A. (2023). A joint monitoring of the process mean and variance with a TEWMA-Max control chart. *Communications in Statistics-Theory and Methods*, *52*(22), 8069-8095. https://doi.org/10.1080/03610926.2022.2056748
[10] Teoh, J. W., Teoh, W. L., Khoo, M. B. C., Celano, G., & Chong, Z. L. (2023). Optimal designs of the omnibus SPRT control chart for joint monitoring of process mean and dispersion. *International Journal of Production Research*. In Press. https://doi.org/10.1080/00207543.2023.2254855
[11] Mahadik, S. B., Godase, D. G., & Teoh, W. L. (2021). A two-sided SPRT control chart for process dispersion. *Journal of Statistical Computation and Simulation*, *91*(17), 3603-3614. https://doi.org/10.1080/00949655.2021.1943667
[12] Deore, R. E., Mahadik, S. B., & Godase, D. G. (2023) The two-sided SPRT sign charts. *Quality and Reliability Engineering International*. In Press. https://doi.org/10.1002/qre.3451
[13] Mahadik, S. B., & Godase, D. G. (2023). A two-sided SPRT control chart for process mean. *Journal of Statistical Computation and Simulation*. In Press. https://doi.org/10.1080/00949655.2023.2296928
[14] Li, J., Yu, D., Song, Z., Mukherjee, A., Chen, R., & Zhang, J. (2022). Comparisons of some memory-type control chart for monitoring Weibull-distributed time between events and some new results. *Quality and Reliability Engineering International*, *38*(7), 3598-3615. https://doi.org/10.1002/qre.3154
[15] Hashim, M. Y., Amin, A. M., Marwah, O. M. F., Othman, M. H., Hanizan, N. H., & Norman, M. K. E. (2020). Two parameters Weibull analysis on mechanical properties of kenaf fiber under various conditions of alkali

treatment. *International Journal of Integrated Engineering*, *12*(3), 245-252. https://doi.org/10.30880/ijie.2020.12.03.028
[16] Paliwal, P. (2021). A technical review on reliability and economic assessment framework of hybrid power system with solar and wind based distributed generators. *International Journal of Integrated Engineering*, *13*(6), 233-252. https://doi.org/10.30880/ijie.2021.13.06.021
[17] Purnomo, M. R. A., Wahab, D. A., & Singh, S. (2023). Optimisation of capacitated planned preventive maintenance in multiple production lines using optimisation-in-the-loop simulation. *International Journal of Integrated Engineering*, *15*(5), 263-272. https://doi.org/10.30880/ijie.2023.15.05.028
[18] Teoh, W. L., Yeong, W. C., Khoo, M. B. C., & Teh, S. Y. (2016). The performance of the double sampling $\bar{X}$ chart with estimated parameters for skewed distributions. *Academic Journal of Science*, *5*(1), 237-52.
[19] Ahmed, A., Sanaullah, A., & Hanif, M. (2020). A robust alternate to the HEWMA control chart under non-normality. *Quality Technology & Quantitative Management*, *17*(4), 423-447. https://doi.org/10.1080/16843703.2019.1662218
[20] Nawaz, M. S., Azam, M., & Aslam, M. (2021). EWMA and DEWMA repetitive control charts under non-normal processes. *Journal of Applied Statistics*, *48*(1), 4-40. https://doi.org/10.1080/02664763.2019.1709809
[21] Godase, D. G., Mahadik, S. B., & Rakitzis, A. C. (2022). The SPRT control charts for the Maxwell distribution. *Quality and Reliability Engineering International*, *38*(4), 1713-1728. https://doi.org/10.1002/qre.3047
[22] Mahadik, S. B., & Godase, D. G. (2023). The SPRT sign chart for process location. *Communications in Statistics-Theory and Methods*, *52*(7), 2276-2290. https://doi.org/10.1080/03610926.2021.1949474
[23] Gorgin, V., & Sadeghpour Gildeh, B. (2020). MAD control chart for autoregressive models with skew-normal distribution. *Stochastics and Quality Control*, *35*(1), 17-23. https://doi.org/10.1515/eqc-2019-0006
[24] Morales, V. H., & Panza, C. A. (2022). Control charts for monitoring the mean of skew-normal samples. *Symmetry*, *14*(11), 2302. https://doi.org/10.3390/sym14112302
[25] Rinne, H. (2008). *The Weibull Distribution: A Handbook*. CRC Press.